확률론적 파괴역학 및 Size Effect Law에 적용을 위한 다중 균열 구조물에서의 에너지 해방률의 고차 미분값 계산

Computation of the Higher Order Derivatives of Energy Release Rates in a Multiply Cracked Structure for Probabilistic Fracture Mechanics and Size Effect Law

황 찬 규†
Hwang, Changyu

(논문접수일 : 2008년 4월 7일 ; 심사종료일 : 2008년 5월 6일)

요 지

본 논문에서는 다중 균열 구조물에서의 균열 진전에 따른 에너지 해방율 및 고차 미분값을 구할 수 있는 가상균열 진전법을 제시한다. 이 방법은 다중 균열 체계의 에너지 해방율과 고차 미분값이 단 한번의 해석으로 수행될 수 있는 장점이 있다. 예제에서 얻어진 해의 최대 오차는 에너지 해방율 0.2%, 일차 미분값 2~3%, 이차 미분값 5~10%이다. 이 방법으로 구한 에너지 해방률의 미분값들은 파괴 확률을 구하거나, size effect law에 적용될 수 있다.

핵심용어 : 가상균열 진전법, 에너지 해방률의 2차 도함수, 보편적 크기효과법칙, 확률파괴역학해석

Abstract

In this paper, we further generalize the work of Lin and Abel to the case of the first and the second order derivatives of energy release rates for two-dimensional, multiply cracked systems. The direct integral expressions are presented for the energy release rates and their first and second order derivatives. The salient feature of this numerical method is that the energy release rates and their first and second order derivatives can be computed in a single analysis. It is demonstrated through a set of examples that the proposed method gives expectedly decreasing, but acceptably accurate results for the energy release rates and their first and second order derivatives. The computed errors were approximately 0.5% for the energy release rates, 3~5% for their first order derivatives and 10~20% for their second order derivatives for the mesh densities used in the examples. Potential applications of the present method include a universal size effect model and a probabilistic fracture analysis of cracked structures.

Keywords : *virtual crack extension method, second order derivative of energy release rates, universal size effect model, probabilistic fracture mechanics analysis*

1. Introduction

This paper introduces the numerical method able to calculate the energy release rates and their higher order derivatives for a multiply cracked structure. The derivatives of energy release rate can provide useful information for diverse problems: the prediction of stability and arrest of a single crack(Alvarado *et al.*, 1989), the growth pattern analysis of a system of interacting cracks(Nemat-Nasser *et al.*, 1978), configurational stability analysis of evolving cracks(Gao and Rice, 1989), probabilistic fracture mechanics analysis(Rahman and Rao, 2002) and universal size effect model(Bazant, 1995 ; 1997). Several methods have been proposed for calculating the derivative of energy release rate. Sumi and his co-workers(Sumi *et*

† 책임저자, 정회원 · 서울벤처정보대학원대학교 유비쿼터스시스템학과 교수
Tel: 02-3470-5281 ; Fax: 02-523-6767
E-mail: changyu.hwang@gmail.com

• 이 논문에 대한 토론을 2008년 10월 31일까지 본 학회에 보내주시면 2008년 12월호에 그 결과를 게재하겠습니다.

al., 1980) presented a combined analytical and finite-element solution method in which special singular crack-tip elements were used. Those singular elements are generated as a result of the second differentiation of potential energy and produce the higher order singularity at the crack-tip. Nguyen and his co-workers(Nguyen, 1990) introduced an explicit expression for the matrix of the second order derivatives of energy with respect to the crack lengths in terms of path independent integrals. A double virtual crack extension method have been presented for the calculation of the second variation of energy for interacting two-dimensional(2-D) linear cracks (Suo and Combescure, 1992). Lin and Abel(Lin, 1988) introduced an analytical virtual crack extension method that uses variational theory in the finite element formulation. The method provides the direct integral forms of energy release rate and its higher order derivatives for a structure containing a single 2-D crack. The method have been generalized to the multiply crack system in 2-D and 3-D(Hwang, 1998 ; 2001). In this paper, the analytical virtual crack extension method is further extended for the calculation of the first and the second order derivatives of energy release rates in a 2-D multiply cracked structure. In Section 2, the general formulation for the higher order derivatives of energy release rates in the multiple crack systems is presented. In Section 3, two example problems are solved to demonstrate the accuracy of the present method. Section 4 discusses the potential application to the universal size effect model and probabilistic fracture analysis of linear-elastic cracked structures.

2. Formulation

In this section, the analytical expressions for derivatives of energy release rates for a multiply cracked system modeled using finite element method are derived. The general formulation, first shown in (Hwang, 1998), is first repeated here for convenience. Next, the new formulation for the second order derivatives of energy release rates in multiply cracked systems is presented. For all the developments reported herein, it is assumed that each crack tip will be surrounded by a symmetric rosette of standard, quarter-point singular elements, as shown in Figure 1.

2.1 General formulation for the first and the second order derivatives of energy release rates for multiple crack systems

The potential energy Π of a cracked body with multiple cracks is given by

$$\Pi = \frac{1}{2}u^T K u - u^T f \tag{1}$$

where u, K and f are the nodal displacement vector, the structural stiffness matrix and the applied nodal force vector, respectively. The energy release rate at crack tip i can be expressed as

$$G_i = -\frac{\delta\Pi}{\delta a_i} = -\frac{1}{2}u^T \frac{\delta K}{\delta a_i}u + u^T \frac{\delta f}{\delta a_i} \tag{2}$$

where a_i is the length of crack i, and nonzero contributions to $\delta K / \delta a_i$ and $\delta f / \delta a_i$ occur only over elements adjacent to the crack tip.

It is noted that whenever crack-face, thermal and

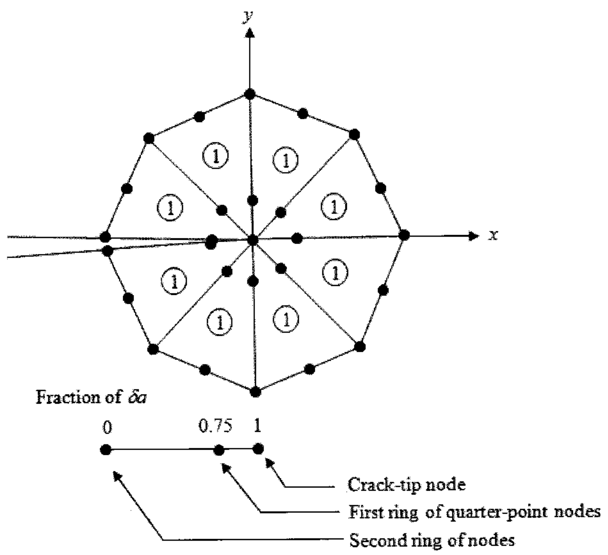

Figure 1 The uniform rosette of standard, quarter-point elements and mesh perturbation of the first ring of crack-tip singular elements.

body force loadings are applied, the variations of loading must be taken into account to reflect the local load change on the crack-face or in the crack tip vicinity as a result of virtual crack extension. The variation of G_i, Eq. (2), with respect to the growth of any other crack, j, is,

$$\frac{\delta G_i}{\delta a_j}=-u^T\frac{\delta K}{\delta a_i}\frac{\delta u}{\delta a_j}-\frac{1}{2}u^T\frac{\delta^2 K}{\delta a_i\delta a_j}u+\frac{\delta u}{\delta a_j}^T\frac{\delta f}{\delta a_i}+u^T\frac{\delta^2 f}{\delta a_i\delta a_j} \tag{3}$$

The second variation of G_i, Eq. (2), with respect to the growth of any other cracks, j and k, is,

$$\begin{aligned}\frac{\delta^2 G_i}{\delta a_j\delta a_k}=&-\frac{\delta u}{\delta a_k}^T\frac{\delta K}{\delta a_i}\frac{\delta u}{\delta a_j}-u^T\frac{\delta^2 K}{\delta a_i\delta a_k}\frac{\delta u}{\delta a_j}\\&-u^T\frac{\delta K}{\delta a_i}\frac{\delta^2 u}{\delta a_j\delta a_k}-\frac{1}{2}\frac{\delta u}{\delta a_k}^T\frac{\delta^2 K}{\delta a_i\delta a_j}u\\&-\frac{1}{2}u^T\frac{\delta^3 K}{\delta a_i\delta a_j\delta a_k}u-\frac{1}{2}u^T\frac{\delta^2 K}{\delta a_i\delta a_j}\frac{\delta u}{\delta a_k}\\&+\frac{\delta^2 u}{\delta a_j\delta a_k}^T\frac{\delta f}{\delta a_i}+\frac{\delta u}{\delta a_j}^T\frac{\delta^2 f}{\delta a_i\delta a_k}\\&+\frac{\delta u}{\delta a_k}^T\frac{\delta^2 f}{\delta a_i\delta a_j}+u^T\frac{\delta^3 f}{\delta a_i\delta a_j\delta a_k}\end{aligned} \tag{4}$$

The variation of the displacement can be obtained from the variation of the global equilibrium equation $Ku=f$ with respect to a_j,

$$\frac{\delta K}{\delta a_j}u+K\frac{\delta u}{\delta a_j}=\frac{\delta f}{\delta a_j}$$
$$\text{or}\quad \frac{\delta u}{\delta a_j}=K^{-1}\left(\frac{\delta f}{\delta a_j}-\frac{\delta K}{\delta a_j}u\right) \tag{5}$$

The second variation of the displacement is

$$\frac{\delta^2 u}{\delta a_j\delta a_k}=K^{-1}\begin{pmatrix}\frac{\delta^2 f}{\delta a_j\delta a_k}-\frac{\delta^2 K}{\delta a_j\delta a_k}u\\-\frac{\delta K}{\delta a_j}\frac{\delta u}{\delta a_k}-\frac{\delta K}{\delta a_k}\frac{\delta u}{\delta a_j}\end{pmatrix} \tag{6}$$

We assume that the elements influenced by each crack-tip in a multiply cracked body comprise disjoint sets. Therefore, if $i\neq j$, then the second order variations of stiffness and loading with respect to two different crack extensions, a_i and a_j, vanish,

$$\frac{\delta^2 K}{\delta a_i\delta a_j}=\frac{\delta^2 f}{\delta a_i\delta a_j}=0 \tag{7}$$

Hence, when $i\neq j$, the first order derivative of energy release rate with respect to two different crack extensions a_i and a_j is given as

$$\frac{\delta G_i}{\delta a_j}=-u^T\frac{\delta K}{\delta a_i}\frac{\delta u}{\delta a_j}+\frac{\delta u}{\delta a_j}^T\frac{\delta f}{\delta a_i} \tag{8}$$

For $i=j$,

$$\frac{\delta G_i}{\delta a_i}=-u^T\frac{\delta K}{\delta a_i}\frac{\delta u}{\delta a_i}-\frac{1}{2}u^T\frac{\delta^2 K}{\delta a_i^2}u+\frac{\delta u}{\delta a_i}^T\frac{\delta f}{\delta a_i}+u^T\frac{\delta^2 f}{\delta a_i^2} \tag{9}$$

When $i\neq j\neq k$, the second and third order variations of stiffness and loads are null,

$$\frac{\delta^2 K}{\delta a_i\delta a_j}=\frac{\delta^2 K}{\delta a_i\delta a_k}=\frac{\delta^3 K}{\delta a_i\delta a_j\delta a_k}=\frac{\delta^2 f}{\delta a_i\delta a_j}=\frac{\delta^2 f}{\delta a_i\delta a_k}=\frac{\delta^3 f}{\delta a_i\delta a_j\delta a_k}=0 \tag{10}$$

and the second order derivatives of displacements are

$$\frac{\delta^2 u}{\delta a_j\delta a_k}=K^{-1}\left(-\frac{\delta K}{\delta a_j}\frac{\delta u}{\delta a_k}-\frac{\delta K}{\delta a_k}\frac{\delta u}{\delta a_j}\right) \tag{11}$$

Therefore, the second order derivatives of energy release rates are given by

$$\frac{\delta^2 G_i}{\delta a_j\delta a_k}=-\frac{\delta u}{\delta a_k}^T\frac{\delta K}{\delta a_i}\frac{\delta u}{\delta a_j}$$

$$-u^T \frac{\delta K}{\delta a_i}\frac{\delta^2 u}{\delta a_j \delta a_k} + \frac{\delta^2 u}{\delta a_j \delta a_k}^T \frac{\delta f}{\delta a_i} \tag{12}$$

Element stiffness variations $\delta k_e / \delta a$, $\delta^2 k_e / \delta a^2$ and $\delta^3 k_e / \delta a^3$ are assembled to produce the global stiffness variations $\delta k_e / \delta a$, $\delta^2 k_e / \delta a^2$ and $\delta^3 k_e / \delta a^3$. The element stiffness variations are given by,

$$\delta k_e = \int_v \left[\delta B^T DB + B^T D\delta B + Tr(\tilde{\varepsilon}) B^T DB \right] dV \tag{13}$$

$$\delta^2 k_e = \int_v \left[\delta^2 B^T DB + 2\delta B^T D\delta B + B^T D\delta^2 B \right] dV + \int_v \left[2|\tilde{\varepsilon}| B^T DB + 2Tr(\tilde{\varepsilon})\left(\delta B^T DB + B^T D\delta B \right) \right] dV \tag{14}$$

$$\delta^3 k_e = \int_v \begin{bmatrix} \delta^3 B^T DB + 3\delta^2 B^T D\delta B \\ +3\delta B^T D\delta^2 B + B^T D\delta^3 B \end{bmatrix} dV + 3\int_v \begin{bmatrix} \delta^2 B^T DB + 2\delta B^T D\delta B \\ +B^T D\delta^2 B \end{bmatrix} Tr(\tilde{\varepsilon})\, dV + \int_v \begin{bmatrix} 6|\tilde{\varepsilon}|\left(\delta B^T DB + B^T D\delta B \right) \\ +2|\tilde{\varepsilon}| B^T DB + +2|\tilde{\varepsilon}| Tr(\tilde{\varepsilon}) B^T DB \end{bmatrix} dV \tag{15}$$

where $\tilde{\varepsilon}$ is the virtual strain-like matrix, B is the strain-nodal displacement matrix, and D the elastic constitutive matrix. $\tilde{\varepsilon}$ is defined as,

$$\tilde{\varepsilon} = J^{-1} \begin{Bmatrix} \dfrac{\partial N}{\partial \xi^1} \\ \dfrac{\partial N}{\partial \xi^2} \end{Bmatrix} \left\lfloor \Delta_n^1 \quad \Delta_n^2 \right\rfloor = \begin{bmatrix} \tilde{\varepsilon}_{11} & \tilde{\varepsilon}_{12} \\ \tilde{\varepsilon}_{21} & \tilde{\varepsilon}_{22} \end{bmatrix} \tag{16}$$

where Δ's are the geometry changes of the elements due to virtual crack extension and N is the standard shape function. The described formulation has been implemented in the fracture analysis code, FRANC2D, a 2-D finite-element-based code for simulating crack propagation(Wawrzynek and Ingraffea, 1987). This code performs automatic crack propagation simulation under Linear Elastic Fracture Mechanics(LEFM) conditions.

3. Numerical examples

3.1 Example 1. A center cracked infinite plate subjected to a uniform remote tensile stress: Verification for the single crack case

The first numerical example investigates a central crack in a large plate subjected to uniform remote tensile stress, σ_0. As shown in Figure 2, the initial crack length to width ratio a/W is 0.01 to approximate a central crack in the infinite plate under a plane stress condition. For a direct comparison with analytical solutions for a single crack, only one-half of the plate was modeled, using the symmetry in the problem, with about 500 linear strain triangular elements including quarter-point elements at the cracktip(Figure 3).

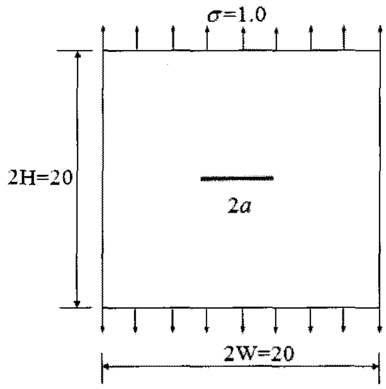

Figure 2 A central crack in a simulated infinite plate under remote unit tensile stress. Not to scale: initial a/W = 0.01, 2H=2W=20*m*, σ_0=1*Pa*. Example 1

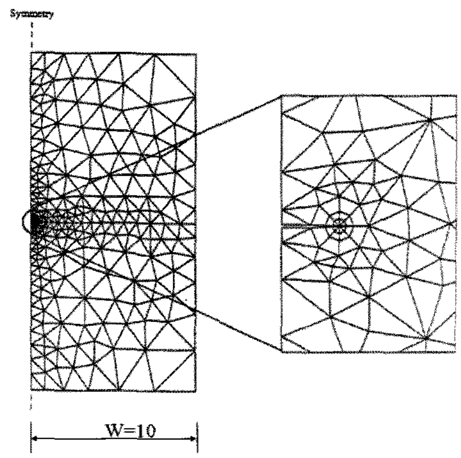

Figure 3 Finite element mesh for a central crack, Example 1.

It should be noted that $\delta f / \delta a$ and $\delta^2 f / \delta a^2$ terms are null for a virtual crack extension under this loading. This model is analyzed to demonstrate the capability of the proposed method for evaluating the second derivative of mode-I energy release rate and stress intensity factor. The exact solutions of K_I, $\delta K_I / \delta a$ and $\delta^2 K_I / \delta a^2$for a mode-I crack under uniform remote tensile stress, σ_0, in an infinite plate can be expressed analytically as(Paris and Sih, 1965),

$$K_I = \sigma_0 \sqrt{\pi a}\ ,\ \frac{\delta K_I}{\delta a} = \frac{\sigma_0}{2}\sqrt{\frac{\pi}{a}}\ ,\ \frac{\delta^2 K_I}{\delta a^2} = -\frac{\sigma_0}{4a}\sqrt{\frac{\pi}{a}} \tag{17}$$

Tables 1, 2 and 3 show that the best computed solutions differ from the exact by about 0.1% for K_I, 2-3% for $\delta K_I / \delta a$, and 5-10% for $\delta^2 K_I / \delta a^2$, respectively, for the particular value of crack-tip element size used(see Figure 3).

Table 1 Comparison of computed with exact solutions for K_I, Example 1, σ_0=1Pa, 2W=2H=20m, Crack-tip element size=a / 8.

a/W	K_I exact	K_I computed(Error %)
0.10	0.5605	0.5610(0.09)
0.11	0.5879	0.5884(0.08)
0.12	0.6140	0.6145(0.08)
0.13	0.6391	0.6395(0.06)
0.14	0.6632	0.6627(0.08)

Table 2 Comparison of computed with exact solutions for $\delta K_I / \delta a$, Example 1.

a/W	δK_I exact	δK_I computed(Error %)
0.10	2.802	2.739(2.25)
0.11	2.672	2.617(2.06)
0.12	2.558	2.561(1.17)
0.13	2.458	2.404(2.20)
0.14	2.369	2.313(2.36)

Table 3 Comparison of computed with exact solutions for $\delta^2 K_I / \delta a^2$, Example 1.

a/W	Exact	Present solution(Error %)
0.10	-14.012	-15.044(7.37)
0.11	-12.145	-11.637(4.18)
0.12	-10.659	-11.915(11.8)
0.13	-9.454	-9.881(4.52)
0.14	-8.459	-8.911(5.34)

3.2 Example 2. Radial multiple cracks embedded in the infinite plate

The second example problem is a set of radial cracks embedded in an infinite plate subjected to the normal stress σ_{yy}=1Pa, as shown in Figure 4. Two cracks are located along two different local radial axes at distance d=1 from the origin and the length of each crack is taken to be 2a=2m. The orientation of crack 1 is kept constant at 30 deg while the orientation of the second crack is changed from 45 to 60 degrees. Figure 5 shows a finite element discretization for the case of $\theta_1 = 30°$ and $\theta_2 = 60°$. The numerical studies are presented for the normalized energy release rates, and their derivatives, where μ is a shear modulus, $G_0 = k_0 \pi (1+\kappa)/8\mu$, $k_0 = \sigma_{22}\sqrt{a}$, and κ is defined as

$$\kappa = 3 - 4\nu \text{ for plane strain,}$$
$$\kappa = \frac{3-\nu}{1+\nu} \text{ for plane stress.} \tag{18}$$

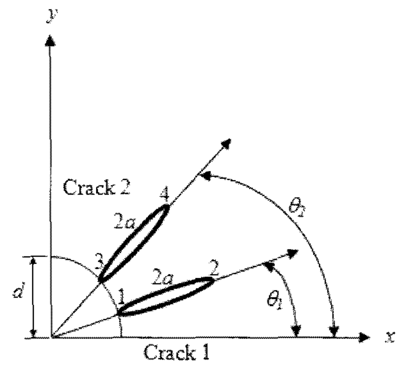

Figure 4 Radial multiple cracks embedded in the infinite plate, d=1m, Example 2

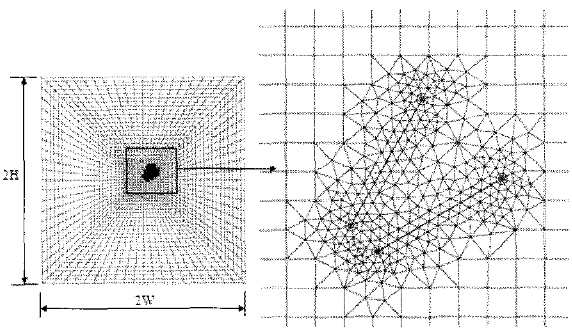

Figure 5 Finite element discretization for radial multiple cracks embedded in the infinite plate (2H=2W=40m), Example 2.

Shear modulus and Poisson's ratio are chosen to be 0.5 and zero, respectively, for this calculation. Therefore, $k_0 = 1$ and $G_0 = \pi$. In this example, cracktip element size is a/6 and three rings of elements are used around the crack-tip for the mesh perturbation. Table 4 compares the normalized energy release rates calculated by the present method with

Table 4 Comparison between numerical and analytical solutions for the normalized energy release rate, G_i / G_0, $\theta_1 = 30°$, Example 2.

	Present Solution		Analytic solution	
Crack tip	$\theta_2 = 45°$	$\theta_2 = 60°$	$\theta_2 = 45°$	$\theta_2 = 60°$
1	0.246	0.539	0.255	0.536
2	0.805	0.802	0.796	0.795
3	0.541	0.292	0.540	0.289
4	0.083	0.076	0.085	0.076

Table 5 The calculated values of the first order derivatives of normalized energy release rates, $\delta G_i / (\delta a_j G_0)$, by the present virtual crack extension method and the finite difference approximation, $\theta_1 = 30°$ and $\theta_2 = 60°$, Example 2.

	Present solution					Finite difference solution					
	1	2	3	4	Row sum		1	2	3	4	Row sum
1	0.418	0.350	-0.289	-0.122	0.357	1	0.420	0.347	-0.290	-0.124	0.353
2	0.350	0.442	0.083	-0.043	0.832	2	0.350	0.462	0.086	-0.041	0.857
3	-0.289	0.083	0.454	0.070	0.318	3	-0.277	0.089	0.455	0.073	0.340
4	-0.122	-0.043	0.070	0.052	-0.043	4	-0.115	-0.041	0.070	0.051	-0.035

Table 6 The calculated values of the second order derivatives of normalized energy release rates, $\delta G_i^2 / (\delta a_j \delta a_k G_0)$, by the present numerical method and the finite difference approximation, $\theta_1 = 30°$and $\theta_2 = 60°$, Example 2.

Present solution					Finite difference solution				
k=1 : $\delta G_i^2 / (\delta a_j \delta a_1 G_0)_{VCE}$					k=1 : $\delta G_i^2 / (\delta a_j \delta a_1 G_0)_{FDM}$				
	1	2	3	4		1	2	3	4
1	1.736	0.059	-1.480	0.087	1	1.299	0.047	-1.484	0.093
2	0.059	-0.064	-0.111	0.042	2	0.047	-0.038	-0.111	0.043
3	-1.480	-0.111	0.930	-0.072	3	-1.484	-0.111	0.863	-0.073
4	0.087	0.042	-0.072	-0.040	4	0.093	0.043	-0.073	-0.035
k=2 : $\delta G_i^2 / (\delta a_j \delta a_2 G_0)_{VCE}$					k=2 : $\delta G_i^2 / (\delta a_j \delta a_2 G_0)_{FDM}$				
	1	2	3	4		1	2	3	4
1	0.059	-0.064	-0.111	0.042	1	0.064	-0.050	-0.112	0.041
2	-0.064	-0.483	0.037	0.258	2	-0.050	0.020	0.039	0.255
3	-0.111	0.037	0.149	-0.025	3	-0.112	0.039	0.119	-0.023
4	0.042	0.258	-0.025	-0.249	4	0.041	0.255	-0.023	-0.245
k=3 : $\delta G_i^2 / (\delta a_j \delta a_3 G_0)_{VCE}$					k=3 : $\delta G_i^2 / (\delta a_j \delta a_3 G_0)_{FDM}$				
	1	2	3	4		1	2	3	4
1	-1.480	-0.111	0.930	-0.072	1	-1.556	-0.112	0.959	-0.071
2	-0.111	0.037	0.149	-0.025	2	-0.112	0.038	0.148	-0.025
3	0.930	0.149	-0.553	0.017	3	0.959	0.148	-0.576	0.016
4	-0.072	-0.025	0.017	0.008	4	-0.071	-0.025	0.016	0.010
k=4 : $\delta G_i^2 / (\delta a_j \delta a_4 G_0)_{VCE}$					k=4 : $\delta G_i^2 / (\delta a_j \delta a_4 G_0)_{FDM}$				
	1	2	3	4		1	2	3	4
1	0.087	0.042	-0.072	-0.040	1	0.092	0.042	-0.081	-0.039
2	0.042	0.258	-0.025	-0.249	2	0.042	0.260	-0.024	-0.252
3	-0.072	-0.025	0.017	0.008	3	-0.081	-0.024	-0.017	0.009
4	-0.040	-0.249	0.008	0.193	4	-0.039	-0.252	0.009	0.218

analytical solutions(Shbeeb *et al.*, 1999a ; 1999b). The analytical solutions are for multiple cracks in an infinite non-homogeneous plate, but they contain solutions for homogeneous material, which can be used as reference solutions. Table 4 indicates that a good agreement between numerical and analytical solutions was obtained for normalized energy release rate, with about 2-3% differences for the mesh density used in this analysis. For the first order derivatives of energy release rates, finite difference solutions are adopted as reference values for the case of $\theta_1 = 30°$ and $\theta_2 = 60°$. Table 5 compares the first order derivatives of normalized energy release rates by the present method and finite difference approximation. The crack extension increment δa_k used in the finite difference solution was 1% of the half crack length, a. A difference of 5% was observed between the present and finite difference solutions in major diagonal terms.

We obtain finite difference solutions for the second order derivatives of energy release rates by

$$\frac{\delta^2 G_i}{\delta a_j \delta a_k}_{FDM} \cong \frac{1}{\delta a_k}\left[\frac{\delta G_i}{\delta a_j}(a+\delta a_k)_{VCE} - \frac{\delta G_i}{\delta a_j}(a)_{VCE}\right] \qquad (19)$$

where 4-by-4 derivative matrices $\delta G_i / \delta a_j$ are calculated by the present numerical method for five different crack geometries (a_1, a_2, a_3, a_4), $(a_1+\delta a_1, a_2, a_3, a_4)$, $(a_1, a_2+\delta a_2, a_3, a_4)$,$(a_1, a_2, a_3+\delta a_3, a_4)$ and $(a_1, a_2, a_3, a_4+\delta a_4)$. It is shown from Table 6 that the present numerical solutions for the second order derivative of normalized energy release rate are in good agreement with finite difference solutions.

4. Applications

In this section, potential application problems of the present method are discussed.

4.1 Universal Size Effect Model

In the universal size effect model(Bazant 1995 ; 1997), the nominal strength of the structure, σ_N is given by

$$\sigma_N = \sigma_0\left(\frac{D}{D_0}+1-\frac{2D_b}{D}\right)^{-(1/2)} \quad \text{where,}$$

$$\sigma_0 = \sqrt{\frac{EG_f}{c_f g'}},\ D_0 = \frac{c_f g'}{g},\ D_b = \bar{c}_f\frac{\langle g''\rangle}{4g'} \qquad (20)$$

As shown, the nominal strength σ_N is given as a function of structure size D, fracture energy G_f, effective length of fracture process zone c_f, dimensionless energy release rate g and its higher order derivatives, $g'$and g''. The model represents a smooth transition from the case of plasticity, for which there is no size effect, to the case of LEFM, for which the size effect is the strongest possible. The present method can provide the accurate values of energy release rate and its higher order derivatives for universal size effect model.

4.2 First and Second Order Reliability Methods(FORM/SORM) for probabilistic fracture mechanics analysis

In the stochastic approach, the performance of the cracked structure is evaluated using the probability of failure, P_F, defined as

$$P_F \overset{def}{=} P_r\left[H(X)<0\right] \overset{def}{=} \int_{g(x)<0} f_x(x)\,dx \qquad (21)$$

where $f_x(x)$ is the joint probability density function of X. In a cracked structure, X denotes an N-dimensional random vector with crack geometry (a), crack orientation, mode-I fracture energy(G_{Ic}) at crack initiation, and loads. If the propagation of a mode-I crack constitutes a failure condition, the performance function is

$$H(x) = G_{Ic} - G \qquad (22)$$

where $H(x)=0$ means crack propagation. To compute the failure probability in Eq. (21), Rahman and Rao [5] used the FORM which leads to nonlinear constrained optimization, requiring the derivative of the performance function with respect to crack size (a) as

$$\frac{\partial H}{\partial a} = -\frac{\partial G}{\partial a} \tag{23}$$

if fracture energy G_{Ic} is a constant. If the SORM is used, the probabilistic analysis requires the second order derivatives of energy release rate. Then, the second order derivative of the performance function will be given as

$$\frac{\partial^2 H}{\partial a^2} = -\frac{\partial^2 G}{\partial a^2} \tag{24}$$

5. Conclusions

In this paper, the work of Lin and Abel(Lin and Abel, 1988) is further extended to the general case of multiple crack systems. Analytical expressions are presented for energy release rates, and their first and second order derivatives for a multiply cracked body. The salient feature of this approach is that all of these values can be computed in a single finite element analysis. The present method has been implemented and verified in FRANC2D, fracture analysis software developed by the Cornell Fracture Group. It is demonstrated through numerical examples that the proposed method gives expectedly decreasing, but acceptably accurate results for the energy release rates, their first and second order derivatives. The computed errors are about 0.5% for the energy release rates, 2-3% for their first order derivatives and 5-10% for the second order derivatives for the mesh density used in these examples. Potential application problems of the present method include probabilistic fracture mechanics analysis of linear-elastic cracked structures and the universal size effect model both of which require calculation of derivatives of energy release rates.

References

Alvarado, Shah, S.P., John R. (1989) Mode-I fracture in concrete using center-cracked plate specimens, *Journal of Engineering Mechanics*, ASCE 115(2), pp.366~383.

Bazant, Z.P. (1995) Scaling theories for quasi brittle fracture: recent advances and new directions, *Fracture Mechanics of Concrete structures, Proceedings FRAMCOS-2*, edited by Folker H. Wittmann, AEDIFICATIO Publishers, D-79014 Freiburg, pp.515~534.

Bazant, Z.P. (1997) Scaling of quasibrittle fracture: asymptotic analysis, *International Journal of Fracture*, 83, pp.19~40.

Gao, H., Rice, J.R. (1989) A first-order perturbation analysis of crack trapping by arrays of obstables, *Journal of Applied Mechanics*, 56(1989), pp.828~836.

Hwang, C.G., Warwzynek, P.A., Tayebi, A.K., Ingraffea, A.R. (1998) On the virtual crack extension method for calculating rates of energy release rate, *Engineering Fracture Mechanics*, 59 (4), pp.521~542.

Hwang, C.G., Warwzynek, P.A., Ingraffea, A.R. (2001) On the virtual crack extension method for calculating the derivatives of energy release rates for a three-dimensional planar crack of arbitrary shape under mode-I loading, *Engineering Fracture Mechanics*, 68, pp.925~947.

Lin, S.C., Abel, J.F. (1988) Variational approach for a new direct-integration form of the virtual crack extension method, *International Journal of Fracture*, 38, pp.217~235.

Nemat-Nasser, S., Keer, L.M., Parihar, K.S. (1978) Unstable growth of thermally induced interacting cracks in brittle solids, *International Journal of Solids and Structures*, 14, pp.409~430.

Nguyen, Q.S., Stolz, C., Debruyne, G. (1990) Energy methods in fracture mechanics: stability, bifurcation and second variations, *European Journal of Mechanics, A/Solids*, 9(2), pp.157~173.

Paris, P.C., Sih, G.C. (1965) Stress analysis of cracks, ASTM-STP 381, p.65.

Rahman, S., Rao, B.N. (2002) Probabilistic fracture mechanics by Galerkin meshless methods - part II: reliability analysis, *Computational Mechanics*, 28

(5), pp.365~374.

Shbeeb, N.I., Binienda, W.K., Kreider, K.L. (1999a) Analysis of the driving forces for multiple cracks in an infinite nonhomogeneous plate, Part I: theoretical analysis, *ASME Journal of Applied Mechanics*, 66, pp.492~500.

Shbeeb, N.I., Binienda, W.K., Kreider, K.L. (1999b) Analysis of the driving forces for multiple cracks in an infinite nonhomogeneous plate, Part II: numerical solutions, *ASME Journal of Applied Mechanics*, 66, pp.501~506.

Sumi, Y., Nemat-Nasser, S., Keer, L.M. (1980) A new combined analytical and finite-element solution method for stability analysis of the growth of interacting tension cracks in brittle solids, *International Journal of Engineering Science*, 18, pp.211~224.

Suo, X., Combescure, A. (1992) Double virtual crack extension method for crack growth stability assessment, *International Journal of Fracture*, 57, pp.127~150.

Warwzynek, P.A., Ingraffea, A.R. (1987) Interactive Finite Element Analysis of Fracture Processes: An Integrated Approach, *Theoretical and Applied Fracture Mechanics*, 8, pp.137~150.